



HAL
open science

Correlation between magnetic resonance, X-ray imaging alterations and histological changes in an ovine model of age-related disc degeneration

N Bouhsina, C Decante, J B Hardel, S Madec, J Abadie, A Hamel, C Le Visage, J Lesoeur, J Guicheux, J Clouet, et al.

► To cite this version:

N Bouhsina, C Decante, J B Hardel, S Madec, J Abadie, et al.. Correlation between magnetic resonance, X-ray imaging alterations and histological changes in an ovine model of age-related disc degeneration. *eCells and Materials Journal*, 2021, 42, pp.166 - 178. 10.22203/ecm.v042a13 . inserm-03367848

HAL Id: inserm-03367848

<https://inserm.hal.science/inserm-03367848>

Submitted on 6 Oct 2021

HAL is a multi-disciplinary open access archive for the deposit and dissemination of scientific research documents, whether they are published or not. The documents may come from teaching and research institutions in France or abroad, or from public or private research centers.

L'archive ouverte pluridisciplinaire **HAL**, est destinée au dépôt et à la diffusion de documents scientifiques de niveau recherche, publiés ou non, émanant des établissements d'enseignement et de recherche français ou étrangers, des laboratoires publics ou privés.

CORRELATION BETWEEN MAGNETIC RESONANCE, X-RAY IMAGING ALTERATIONS AND HISTOLOGICAL CHANGES IN AN OVINE MODEL OF AGE-RELATED DISC DEGENERATION

N. Bouhsina^{§,1,2,3}, C. Decante^{§,1,2,4}, J.B. Hardel³, S. Madec^{1,3}, J. Abadie^{5,6}, A. Hamel^{1,2,4}, C. Le Visage^{1,2}, J. Lesoeur^{1,2}, J. Guicheux^{*,1,2,7}, J. Clouet^{§,1,8,9} and M. Fusellier^{§,1,2,3}

¹INSERM, UMRS 1229, Regenerative Medicine and Skeleton (RMes), Université de Nantes, ONIRIS, Nantes, F-44042, France

²Université de Nantes, UFR Odontologie, Nantes, F-44042, France

³Department of Diagnostic Imaging, CRIP, ONIRIS, College of Veterinary Medicine, Food Science and Engineering, Nantes, F-44307, France

⁴CHU Nantes, Service de Chirurgie Infantile, PHU5, Nantes, F-44093, France

⁵AMaROC, ONIRIS, College of Veterinary Medicine, Food Science and Engineering, Nantes, F-44307, France

⁶CRCINA, INSERM, Université d'Angers, Université de Nantes, Nantes, France

⁷CHU Nantes, PHU4 OTONN, Nantes, F-44093, France

⁸Université de Nantes, UFR des Sciences Biologiques et Pharmaceutiques, Nantes, F-44042, France

⁹CHU Nantes, Pharmacie centrale, PHU11, Nantes, F-44042, France

§,§ These authors contributed equally to this work

Abstract

Sheep are one of the many animal models used to investigate the pathophysiology of disc degeneration and the regenerative strategies for intervertebral disc (IVD) disease. To date, few studies have thoroughly explored ageing of ovine lumbar IVDs. Hence, the objective of the present study was to concomitantly assess the development of spontaneous age-related lumbar IVD degeneration in sheep using X-ray, magnetic resonance imaging (MRI) as well as histological analyses.

8 young ewes (<48 months old) and 4 skeletally mature ewes (>48 months old) were included. Disc height, Pfirmann and modified Pfirmann grades as well as T2-wsi and T2 times were assessed by X-ray and MRI. The modified Boos score was also determined using histology sections.

Pfirmann (2 to 3) and modified Pfirmann (2 to 4) grades as well as Boos scores (7 to 13) gradually increased with ageing, while T2-weighted signal intensity (1.18 to 0.75), T2 relaxation time (114.36 to 70.65 ms) and disc height (4.1 to 3.2 mm) decreased significantly. All the imaging modalities strongly correlated with the histology ($p < 0.0001$).

The present study described the suitability of sheep as a model of age-related IVD degeneration by correlation of histological tissue alterations with the changes observed using X-ray and MRI. Given the structural similarities with humans, the study demonstrated that sheep warrant being considered as a pertinent animal model to investigate IVD regenerative strategies without induction of degeneration.

Keywords: Intervertebral disc, degeneration, sheep, magnetic resonance imaging, X-ray imaging, histology.

***Address for correspondence:** J. Guicheux, INSERM, UMRS 1229, Regenerative Medicine and Skeleton (RMes), Université de Nantes, ONIRIS, Nantes, F-44042, France.

Telephone number: +33 240412916 Email: jerome.guicheux@inserm.fr

Copyright policy: This article is distributed in accordance with Creative Commons Attribution Licence (<http://creativecommons.org/licenses/by-sa/4.0/>).

List of Abbreviations		CK-18	keratin 18
3Rs	replace, reduce, refine	CT	computer tomography
AB	alcian blue	ECM	extracellular matrix
AF	annulus fibrosus	GAL3	galectin-3
CD24	cluster of differentiation 24	HES	haematoxylin eosin safran
CI	confidence interval	IVD	intervertebral disc
CK-8	keratin 8	LBP	low-back pain
		MDH	midpoint disc height

MR	magnetic resonance
MRI	magnetic resonance imaging
NP	nucleus pulposus
ROI	region of interest
SEM	standard error of the mean
T2-wsi	T2-weighted signal intensity

Introduction

LBP is a major issue not only from a medical perspective but also in terms of its societal and economic impact. Indeed, LBP is one of the most common causes of disability and a significant economic burden (Geurts *et al.*, 2018; Hoy *et al.*, 2014; Kigozi *et al.*, 2019), with an estimated cost of 87.6 billion dollars in 2013 in the United States, making it the third-highest healthcare cost after diabetes and ischemic heart disease (Dieleman *et al.*, 2017). LBP is multifactorial and can be related to changes occurring either in IVD, endplates, facet joints, vertebral bone marrow or spinal muscles. IVD degeneration is thought to be one of the main causes of LBP (Khan *et al.*, 2017) and 266 million individuals worldwide are affected each year by LBP due to degenerative disc disease (Ravindra *et al.*, 2018). LBP due to IVD degeneration is also referred to as discogenic back pain (De Schepper *et al.*, 2010; Luoma *et al.*, 2000). IVD degeneration is defined as an “aberrant cell-mediated response to progressive structural failure” (Adams and Roughley, 2006). Age is one of the main factors associated with degeneration, although various mechanical, genetic, nutritional and environmental factors can mimic the age-related changes that occur in IVDs (Adams and Roughley, 2006). Age-related changes in the IVD correspond to naturally occurring cell senescence, whereas pathological IVD degeneration refers to the precocious modifications in the tissue composition caused by these various factors (Wang *et al.*, 2016). The initiating mechanisms differ between IVD senescence and degeneration but, since they result in the same histological modifications of the IVD tissue, the term “IVD degeneration” is frequently used to define both mechanisms.

In light of the high prevalence of discogenic back pain, it appears essential to understand the complex mechanisms that lead to IVD degeneration. A better understanding of this pathogenesis would help with the development of treatments to reduce the degenerative process, limit its onset or repair damaged IVDs. For this purpose, many *in vitro*, *in vivo* and *ex vivo* studies have been carried out (Alini *et al.*, 2008; Clouet *et al.*, 2019; Fusellier *et al.*, 2020). As the investigation of human tissues can be limited due to the difficulties of obtaining human histological material, preclinical animal models are an attractive option.

Numerous preclinical animal models have been developed to study IVD degeneration and to investigate the changes that occur in the various

structures (AF, NP and endplate) of the IVD and at different levels (cellular, ECM, neurovascular, *etc.*) (Fusellier *et al.*, 2020). The most suitable model has to be ethical and cost-effective and the conditions for the study should be reproducible. Above all, the model has to mimic the pathological features of human IVD as closely as possible (Alini *et al.*, 2008; Singh *et al.*, 2005). To investigate IVD pathophysiology, spontaneous and induced IVD degeneration have been widely used in animal models. Induction of the IVD degeneration can be triggered mechanically (*e.g.* by fusion, with consequent instability of adjacent segments), chemically (*e.g.* by chemonucleolysis) or by injury (*e.g.* by endplate injury, annulotomy or nucleotomy) (Daly *et al.*, 2016). Nevertheless, induction of IVD degeneration is invasive and can be time-consuming, as a considerable amount of time can be required to allow the onset and development of the degenerative process, depending on the induction modality used. For example, discectomy induces IVD degeneration after approximately 6 weeks (Sloan *et al.*, 2020), while instability only induces this degeneration after at least 9 months (Fusellier *et al.*, 2020). Additionally, IVD degeneration triggered by inductive methods can drastically influence the outcomes of the tested regenerative therapies, particularly in case of chemonucleolysis due to residual enzyme activity (Fusellier *et al.*, 2020). Moreover, human IVD degeneration is not always caused by injury, as ageing is one of the main factors involved and many patients diagnosed with IVD degeneration do not exhibit LBP. Consequently, inducing degeneration does not always result in the intended purpose of mimicking the changes that occur naturally in human degenerative IVDs. Thus, age-related spontaneous IVD degeneration animal models appear to be the most appropriate way to investigate this affliction. Spontaneous IVD degeneration has been well described in a number of species [*e.g.* sand rat (Gruber *et al.*, 2002), chondrodystrophic dog (Bergknut *et al.*, 2012), rabbit (Clouet *et al.*, 2011), mouse (Ohnishi *et al.*, 2018), non-human primates such as baboon (Craig Platenberg *et al.*, 2001), macaque (Nuckley *et al.*, 2008) and sheep (Nisolle *et al.*, 2016)]. In this last study, the naturally occurring changes were evaluated by imaging modalities (MRI and CT) but the histological features were not described or correlated to the changes seen by MRI and CT. In addition to anatomical similarities, ovine and human IVDs have also been reported to have common biomechanical and histological features (Daly *et al.*, 2016; Reid *et al.*, 2002; Schmidt and Reitmaier, 2013; Sheng *et al.*, 2010; Wilke *et al.*, 1997a; Wilke *et al.*, 1997b). Therefore, sheep IVDs can be considered to be a pertinent model of human IVD degeneration (Reitmaier *et al.*, 2017). Consequently, the aims of the present study were (i) to assess the age-related spontaneous IVD degeneration in ovine lumbar spine by concomitant use of imaging features (MRI and X-ray) and histological tools; (ii) to determine whether there was a correlation between

Table 1. MRI parameters.

	Sagittal T2-weighted fast spin echo	Axial T2-weighted fast spin echo	T2 mapping
Repetition time (ms)	3,000	6,520	1,510
Echo time (ms)	86	98	13.8/27.6/41.4/55.2/69
Flip angle (°)	120	120	180
Matrix	512 × 512	448 × 448	256 × 264
Section thickness (mm)	3	2.5	3
Number of signals acquired	7	30	7
Bandwidth	200	190	225

the results obtained using the different imaging methods and histology in this species. The authors hypothesised (i) that spontaneous degeneration of the lumbar ovine IVD could be assessed analysing both imaging and histological features and (ii) that imaging correlated with histological scoring of IVD degeneration in the sheep model. If there was such a correlation, the imaging characteristics of IVD degeneration could provide an alternative to systematic histological assessment of degeneration, which would be of considerable relevance in longitudinal studies using sheep as a large animal model.

Materials and Methods

Cohort

12 sheep were used for the study. 8 were skeletally immature female sheep that were less than 48 months old (group 1) and 4 were skeletally mature females that were more than 48 months old (group 2). As epiphyseal fusion of the vertebral bodies occurs at the age of 4 years and is one of the last epiphysial fusions in sheep (Barone, 2010; Moran and O'Connor, 1994), ewes older than 4 years were included in the second group.

The cohort came from an accredited farm (GAEC HEAS farm, Ligné, France). All the sheep underwent distant and close physical, orthopaedic and neurological examinations. To evaluate the presence or absence of LBP and neurological disorders, palpation of the lumbar area was performed and a criterion scale was applied to evaluate the behaviour of and the pain in the sheep. This scale assessed alertness (normal, increased, reduced or lethargic), posture (standing or lying down), standing posture, if applicable (stationary, normal movement, careful movement, movement without flexion of the hindlimbs), head position while standing (normal or low), head position while moving (normal or low), presentation of back and hindlimbs (normal or abnormal, arched back), vocalisation (normal bleating, moaning, cringing), appetite (normal, dysorexia or anorexia), reaction when the operator approached (quick escape, slow escape, no escape). Animals were excluded if they presented any orthopaedic or neurological

disorders. All animal experiments were carried out in accordance with EU Directive 2010/63/EU. The study was approved by the French Ministry of Agriculture and the ethics committee of the Pays de la Loire (Ethics Approval number: CEEA-PDL APAFIS 6170).

X-ray and MRI

Sheep were anaesthetised for the imaging procedures. The anaesthetic protocol included intravenous injections of diazepam (0.2-0.4 mg/kg) and ketamine (2-5 mg/kg) and induction by intravenous injection of propofol (1-3 mg/kg) followed by inhalation of 1-3 % isoflurane.

Plain radiographs of the lumbar spine were taken using a radiography machine (Convix 80 generator[®] and Universix 120[®] table, Picker International, Uniontown, OH, USA). Sagittal and dorsoventral radiographs were performed with a collimator-to-film distance of 1 m, an exposure of 20-30 mAs and a tube voltage of 70-85 kV. Fluoroscopy, included in the radiography equipment, was used to check the absence of rotation (superposition of the ilium wings and crests and of the transverse processes of the lumbar vertebrae).

MRI of the entire lumbar spine was performed using a 1.5 T MR scanner (Magnetom Essenza[®], Siemens Medical Solutions) using a standard body coil to obtain sagittal and axial T2-weighted images and sagittal T2 mapping images. MRI acquisition parameters are listed in Table 1.

Image analysis

Images were analysed using Horos software 3.0[®] (Horos Project, Geneva, Switzerland). X-ray images were used to determine the number of lumbar IVDs, as they vary between 5 and 6 in sheep, and to verify the absence of a major bone disease (congenital malformation of the vertebrae, old fracture, tumour) or spondylodiscitis. The lumbar MDH of all lumbar intervertebral spaces was measured on the sagittal radiographs between the midpoint of the caudal endplate of the cranial vertebra and the midpoint of the cranial endplate of the caudal vertebra as described by Lee *et al.* (2017) (Fig. 1).

Lumbar IVDs were evaluated on T2-weighted sagittal MRI sequences using the five-point Pfirrmann grading system (Pfirrmann *et al.*, 2001), which is based on MR signal intensity, distinction between NP and AF, IVD structure and IVD height. To better

detect the early changes in degenerative IVDs, the modified Pfirrmann grading system was also applied (Griffith *et al.*, 2007). This method is based on eight grades characterised by the signal from the NP and the inner AF compared with the cerebrospinal fluid signal, the distinction between the inner and the outer part of the dorsal AF and the proportion of the reduction in disc height. These two human grading systems have already been applied for ovine IVD evaluation (Daly *et al.*, 2018; Pennicooke *et al.*, 2018). T2-wsi was measured on MR images of a midsagittal slice. This consisted of the ratio of the mean NP signal intensity divided by the mean spinal cord signal intensity, measured at the same IVD level. Finally, for the T2 relaxation time measurements, a ROI that included the NP of each lumbar disc was manually drawn on the sagittal T2-weighted image. This ROI was duplicated onto the corresponding T2 mapping image and the mean T2 relaxation time of the NP was collected.

Pfirrmann grading, modified Pfirrmann grading and T2 relaxation time measurements were acquired from MR images by two independent blinded observers. Five readings of these three parameters were performed by each observer, with a 1-week interval between the readings.

Histological analysis

After having completed the imaging procedures, the animals were euthanised by intravenous injection of 140 mg/kg pentobarbital.

Lumbar IVDs were harvested and fixed using 4 % paraformaldehyde (in phosphate buffered saline, pH = 7.4) for 2 or 3 d. Then, IVDs were placed in a decalcifier solution (Shandon TBD-2 Decalcifier[®], 6,764,004, Thermo Fisher Scientific) for 1 month before being prepared for sectioning following the Kawamoto method (Kawamoto and Shimizu, 2000). They were frozen in isopentane and dry ice before being embedded in SCEM[®] (Section Lab, Hiroshima,

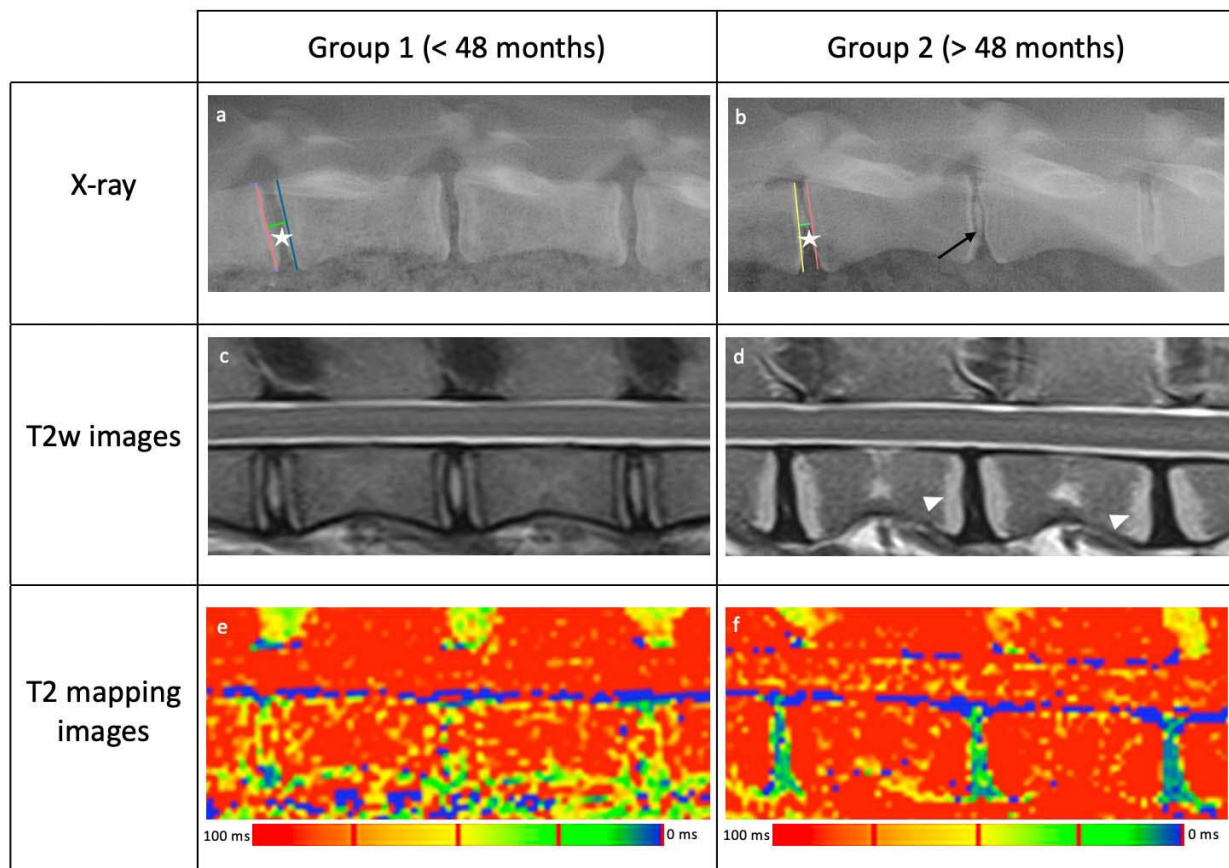


Fig. 1. Sagittal X-ray. T2-weighted sagittal and T2 mapping MR images for the two ovine groups: (a,c,e) group 1 (< 48 months old) and (b,d,f) group 2 (> 48 months old). On the radiographs, the MDH was measured between the middle of the two adjacent endplates (white stars) in (a) groups 1 and (b) 2. One animal in group 2 exhibited NP calcification (black arrow). (c) On the MR images, Pfirrmann grade I was characterised by a homogeneous area, isointense to the cerebrospinal fluid NP, with a clear distinction between this structure and the AF. (d) Grade IV was characterised by an inhomogeneous area, hypointense to the cerebrospinal fluid NP, with a loss of distinction between this structure and the AF. Hyperintensity of the endplates on T2-weighted images and T1-weighted images (data not shown) was present in 3 sheep of group 2. These changes correspond to Modic type 2 changes (white head arrows). T2 relaxation time was measured on T2 mapping images. (e) The NP had a high relaxation time value (> 100 ms), indicated in red on the colour maps, (f) whereas this value was lower in the AF and the degenerated NP (< 50 ms) and is shown in blue or green on the colour maps.

Japan) and frozen again in isopentane and dry ice until the SCEM[®] became fully frozen. Samples were cut at -30°C in an axial orientation into $7\ \mu\text{m}$ -thick slices using a cryostat (CryoStar NX70[®], Thermo Fisher Scientific). Next, they were stained with HES and AB according to a standard protocol (Lucas *et al.*, 2012). If the quality of the sample was considered insufficient to be accurately analysed, it was excluded from the histological analysis. Exclusion criteria corresponded to obtaining partial NP on the slice during the sectioning.

These histological sections were analysed using a modified Boos scoring (Boos *et al.*, 2002) that focuses on the NP. AF and endplates were not assessed. This scoring was based on the analysis of four criteria (decrease in cell density, granular changes, mucous degeneration, tear and cleft formation) and it was aimed at the characterisation of the IVD histomorphology and at the evaluation of the degenerative changes in the ECM. The modified Boos score ranged from 0, which corresponded to a healthy IVD without signs of degeneration, to 22, which corresponded to complete IVD degeneration. Granular and mucous degeneration was ranked from 0 (no changes) to 4 (complete degeneration). Cell death and tear and cleft formation were ranked from 0 to 4. Cell proliferation was ranked from 0 to 6. The lowest score (0) corresponded to an absence of changes and the highest score (4 or 6) corresponded to complete degeneration. Two independent observers performed a blind evaluation of the histological samples. When the score differed by more than two points, the sample was re-examined jointly by the two observers who agreed on a new score that was retained for further analysis. If not, the mean of the two values was used.

Statistical analysis

The statistical analysis was performed using R software (version 4.0.3, The R Foundation, Vienna, Austria). The intra-rater reliability was assessed for the Pfirrmann grading, modified Pfirrmann grading and T2 relaxation time using a linear mixed-effects model. Intra-rater reliability was considered to be high if the value was less than 15 % and moderate if the value was between 16 and 50 %. The weighted kappa coefficient (κ) was used to determine inter-observer reliability for Pfirrmann and modified Pfirrmann gradings. Agreement was excellent for $\kappa > 0.8$, good for $\kappa = 0.6-0.8$, moderate for $\kappa = 0.4-0.6$, fair for $\kappa = 0.2-0.4$ and slight for $\kappa = 0.0-0.2$. For these two parameters, the 5 readings were reviewed and the grade that was assigned the most to each IVD by each observer was retained for the determination of the inter-rater reliability. When the intra-rater reliability was good for the T2 relaxation time, the mean of the 5 values was retained for the calculation of the inter-rater reliability. A coefficient of determination was used to evaluate the inter-rater reliability for the T2 relaxation time. Reliability was considered to be excellent if R^2 was above 0.75, good if R^2 was between

0.6 and 0.75, moderate if R^2 was between 0.4 and 0.59 and poor if R^2 was under 0.4.

All data are presented as medians, SEM and range. Correlations between age and Pfirrmann grades, modified Pfirrmann grades and modified Boos scores were analysed using Spearman correlation tests. Correlations between age and MDH, T2-wsi and T2 relaxation times were analysed using Pearson correlation tests. For these tests, the actual age of each ewe was considered and not the group they had been assigned to and, thus, age was considered as a continuous parameter. Correlations between the histology and each imaging parameter were also studied using Spearman correlation tests. Correlations were considered significant for $p < 0.05$. For all the imaging and histological parameters, significant differences between age groups were assessed using a Wilcoxon Mann-Whitney test. Differences were statistically significant for $p < 0.05$. For every linear mixed-effects model used for the statistical analysis (intra-rater reliability for Pfirrmann grading, modified Pfirrmann grading and T2 relaxation time and correlations between all imaging and histological parameters), normality and independence conditions of the residuals were validated by recommended graphs according to the method described by Pinheiro and Bates (Pinheiro and Bates, 2000) for mixed-effects models.

Results

Cohort

The cohort was composed of 12 Vendée sheep. The mean body weight was 31 kg for group 1 and 73 kg for group 2. The mean age of each group was 20.75 months for group 1 and 90 months for group 2.

The cohort was in good health, except for one animal that exhibited a moderate respiratory impairment. The clinical, orthopaedic and neurological examinations revealed that none of the sheep had a musculoskeletal or neurological disorder or signs of LBP. None of the sheep exhibited a major vertebral disease and, hence, none of the animals were excluded from the study.

Changes in X-ray and MRI parameters

A total of 66 IVDs were studied using imaging modalities. MDH were determined based on X-ray images. MR images were used for the Pfirrmann and modified Pfirrmann grading, as well as to determine T2-wsi and T2 relaxation times. 44 IVDs were assessed in group 1 and 22 in group 2 (animals older than 48 months). In each group, the lumbar spine of half of the animals was composed of 5 IVDs while the other half had 6 IVDs.

Analysis of the intra-rater reliability revealed very strong agreement for the Pfirrmann grading, with intra-rater values of 0.10 and 0.14. Similarly, the T2 relaxation times had very strong intra-rater values of 0.01 and 0.05. The intra-rater reliability

was moderate to poor for the modified Pfirrmann grading, with intra-rater values of 0.27 and 0.88. The inter-rater analysis revealed good agreement for the Pfirrmann grading ($\kappa = 0.64$) and moderate agreement for the modified Pfirrmann grading ($\kappa = 0.54$). The T2 relaxation time measurements had excellent inter-rater reliability ($p < 0.0001$, $R^2 = 0.87$). The slope of the regression line between the two observers did not differ significantly from 1 (0.99; CI = 0.91-1.07) and the line intersect did not differ significantly from 0 (7.49; CI = -1.5-16.48).

The median MDH values decreased from 4.1 mm (SEM: 0.03; range: 1.8) in group 1 to 3.2 mm (SEM: 0.05; range: 1.6) in group 2 (Fig. 1,2). Hyperintense signals of the endplates were observed on both T1- and T2-weighted images in 3/4 of the sheep in group 2 (Fig. 1). These variations in the signal intensity correspond to Modic type 2 changes with fatty marrow replacement in the endplate (Modic *et al.*, 2007). Modic signs were not observed on the endplates of group 1.

The median values of the Pfirrmann score increased from 2 (SEM: 0.07; range: 2) in group 1 to 3 (SEM: 0.06; range: 1) in group 2 (Fig. 3a,b). IVDs of group 1 were mainly rated grade I (13/44) or II (27/44). Only 4 IVDs of these sheep were rated grade III. By contrast, group 2 had IVDs with Pfirrmann grades III (15/22) and IV (7/22). The modified Pfirrmann grades had a similar distribution. The median value increased from 2 (SEM: 0.07; range: 2) in group 1 to 4 (SEM: 0.10; range: 3) in group 2 (Fig. 3c). IVDs of group 1 were mainly rated grade I (10/44) or II (27/44).

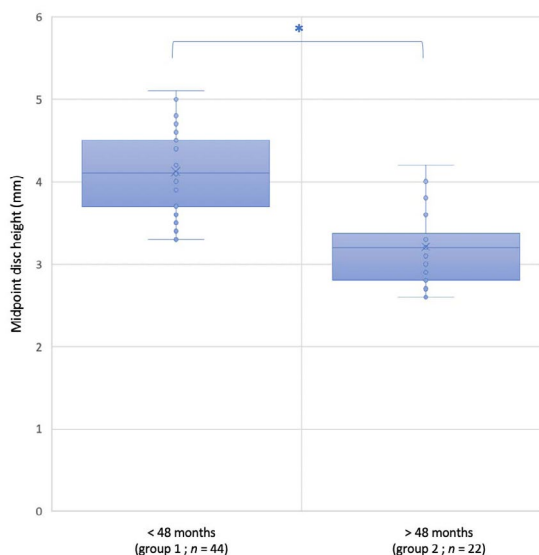


Fig. 2. Variations in MDHs of ovine IVDs between skeletally immature (group 1) and skeletally mature (group 2) sheep. The MDH of each lumbar ovine intervertebral space was measured between the midpoint of the caudal endplate of the cranial vertebra and the midpoint of the cranial endplate of the caudal vertebra. Results are expressed as medians. The correlation between the two groups for MDH values was assessed. * $p < 0.05$, statistical difference between two groups.

7 of the 44 IVDs were rated grade III in group 1. In group 2, IVDs were rated grade III (7/22), IV (9/22), V (4/22) and VI (2/22).

In terms of T2-wsi, values decreased with age. The median T2-wsi value was 1.18 (SEM: 0.02; range: 0.41) and 0.75 (SEM: 0.08; range: 0.92) for groups 1 and 2, respectively (Fig. 4a).

The value of the T2 relaxation time also decreased with age. The median T2 relaxation time value was 114.36 (SEM: 0.57; range: 195.24) and 70.7 (SEM: 0.83; range: 92.3) for groups 1 and 2, respectively (Fig. 4b).

Statistical analysis revealed a significant correlation between:

- age and MDH ($p = 0.014$, $\rho = -0.30$), with statistically significant differences in MDH values between groups 1 and 2 ($p < 0.0001$) (Fig. 2);
- age and Pfirrmann grade ($p < 0.0001$, $r_s = 0.62$), with statistically significant differences between groups 1 and 2 ($p < 0.0001$) (Fig. 3);
- age and modified Pfirrmann grade ($p < 0.0001$, $r_s = -0.67$), with statistically significant differences between groups 1 and 2 ($p < 0.0001$) (Fig. 3);
- age and T2-wsi ($p < 0.0001$, $\rho = 0.82$), with statistically significant differences between groups 1 and 2 ($p < 0.0001$) (Fig. 4a);
- age and T2 relaxation time values ($p < 0.0001$, $\rho = -0.73$), with statistically significant differences between groups 1 and 2 ($p < 0.0001$) (Fig. 4b).

Histological analyses

Individual modified Boos scores based on histological analysis were determined for 56/66 IVDs (group 1: $n = 35/44$; group 2: $n = 21/22$). 9 IVDs from group 1 and 1 IVD from group 2 were removed from histological analysis because of poor quality at the end of the histological procedures. IVDs of group 1 were characterised by a low value for the modified Boos score and the ECM appeared to be well organised, with numerous nucleopulpcytes (Fig. 5a i,ii). Moreover, neither granular changes, mucous degeneration nor tears were observed. In some IVDs of group 1, the modified Boos score increased slightly and nucleopulpcytes proliferation resulted in the formation of clusters that were randomly distributed in the NP (Fig. 5a iii,iv). Analogous to the mucous degeneration, there was a big increase in granular changes between the sheep of group 1 and group 2. In group 2, tears and clefts were observed in some of the IVDs, while numerous empty cells were also noted (referred to as "ghost cells"), which were assumed to reflect cell death (Fig. 5a v,vi). Well-defined nests with clusters of large cells exhibiting large intracellular vacuoles and amorphous nuclei resembling notochordal cells were identified in the central NP of group 1 IVDs. Modified Boos scores increased with age, with a variation from 3 to 9 in group 1 (median value: 7; SEM: 0.11; range: 6) and from 9 to 19 in group 2 (median value: 13; SEM: 0.19; range: 10) (Fig. 5b). Statistical analysis revealed a significant correlation between age and Boos score ($p < 0.0001$, $r_s = 0.77$). Modified Boos scores were

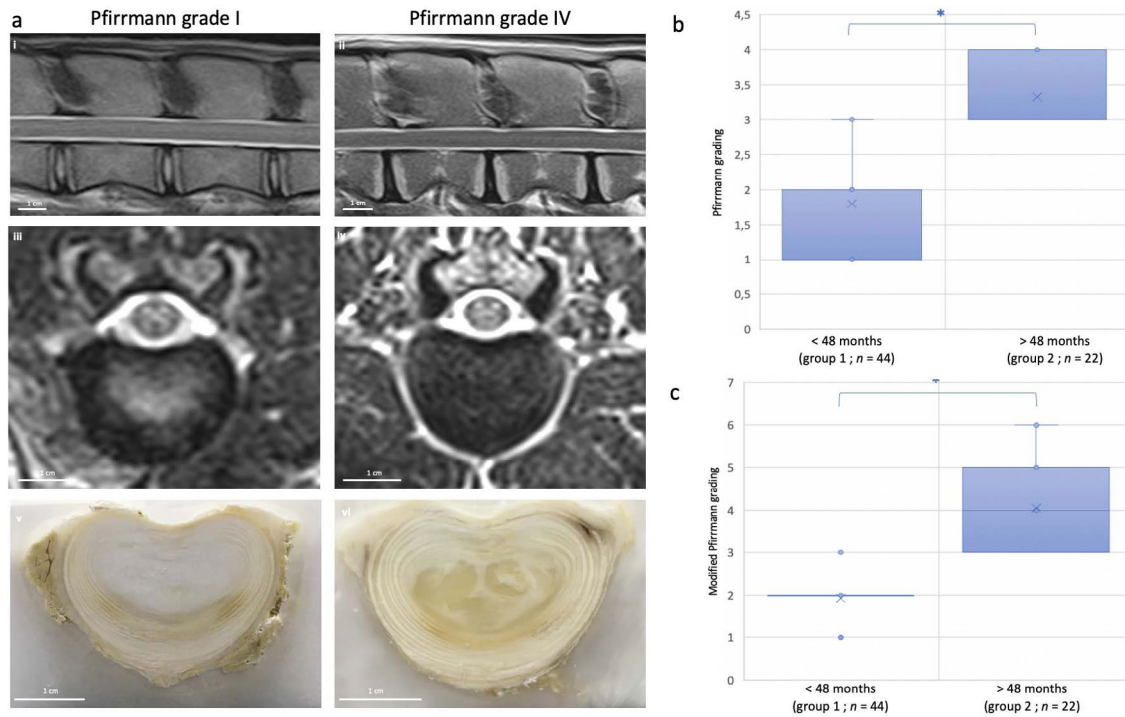


Fig. 3. Assessment of ovine age-related IVD degeneration using MRI Pfirrmann and modified Pfirrmann grading. (a) T2-weighted sagittal and axial MR images and an axial slice of a lumbar ovine IVD classified as Pfirrmann (i,iii,v) grade I from group 1 (< 48 months old) and (ii,iv,vi) grade IV from group 2 (> 48 months old). When the MRI signal of the NP of the degenerated disc was absent, its gross anatomy was (vi) inhomogeneous in contrast to (v) a healthy disc. Graphs represent the variations in (b) Pfirrmann grading and (c) modified Pfirrmann grading between skeletally immature (group 1) and skeletally mature (group 2) sheep. Results are expressed as medians. Correlations between the two groups for Pfirrmann and modified Pfirrmann gradings values were assessed (* $p < 0.05$, statistical difference between two groups).

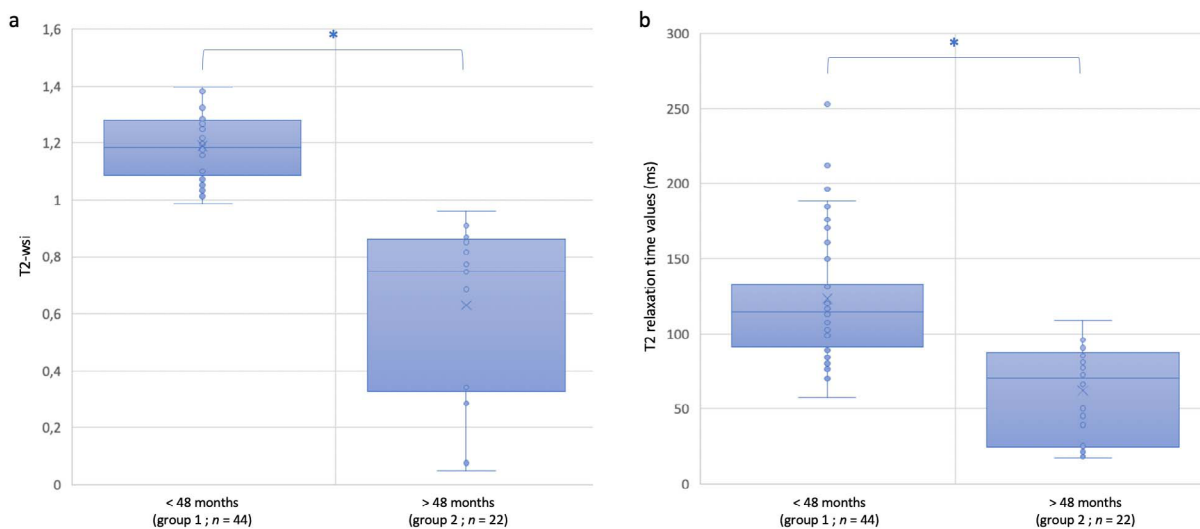


Fig. 4. Variations (a) in T2-wsi and (b) T2 relaxation time values of ovine IVDs between skeletally immature (group 1) and skeletally mature (group 2) sheep. The T2-wsi was measured on MR images of a midsagittal slice. (a) T2-wsi represented the ratio of the mean NP signal intensity divided by the mean spinal cord signal intensity measured at the corresponding ovine IVD level. It was measured on MR sagittal T2-weighted images. (b) Mean T2 relaxation time of the NP was measured by manually drawing a ROI that included the NP of each lumbar ovine disc on the sagittal T2-weighted image and by copying this ROI onto the corresponding T2 mapping image. Results are expressed as medians. Correlations between the two groups for T2-wsi and T2 relaxation time values were assessed. * $p < 0.05$, statistical difference between two groups.

significantly increased between groups 1 and 2 (Fig. 5b).

A positive correlation was found between modified Boos scores and Pfirrmann ($p < 0.0001$, $r_s = 0.84$) and modified Pfirrmann grades ($p < 0.0001$, $r_s = 0.82$) (Fig. 6). Similarly, a negative correlation was found between Boos scores and MDH ($p < 0.0001$, $r_s = 0.52$), T2-wsi ($p < 0.0001$, $r_s = 0.70$) and T2 mapping ($p < 0.0001$, $r_s = 0.52$).

Discussion

The present study evaluated the correlation between MDH on X-rays, MRI and histological characteristics to assess age-related spontaneous lumbar IVD degeneration in sheep. By showing a strong correlation between age, imaging and histological parameters, the present investigation validated the hypothesis that lumbar IVD age-related degeneration

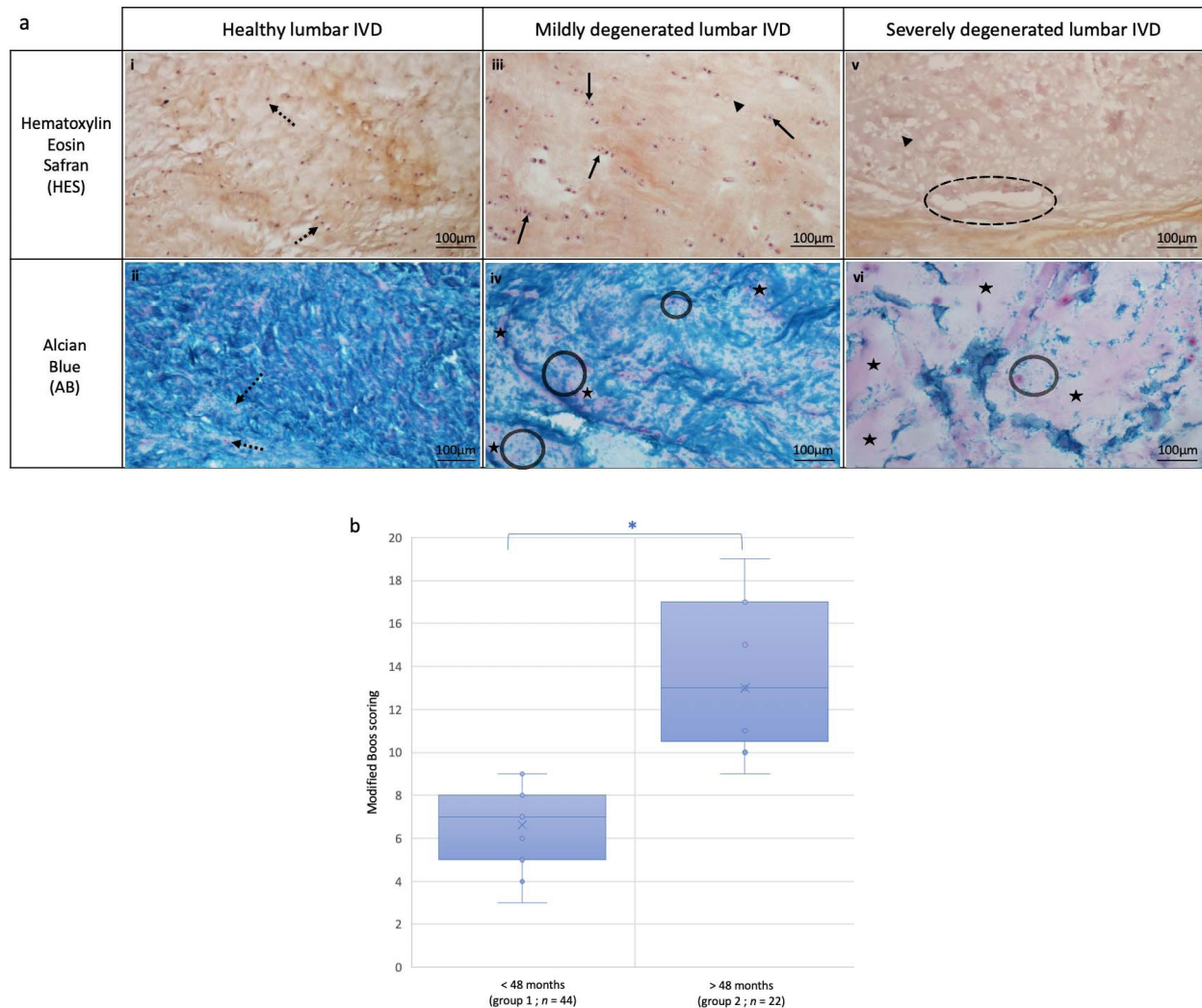


Fig. 5. Histological assessment of age-related NP degeneration in sheep. (a) Histological analysis of lumbar ovine IVDs by (i,iii,v) HES and (ii,iv,vi) AB staining according to the different grades of degeneration: (i,ii) healthy lumbar ovine disc with a Boos score of 4; (iii,iv) mildly degenerated lumbar ovine disc with a Boos score of 9; (v,vi) severely degenerated lumbar ovine disc with a Boos score of 19. In healthy IVDs, the round nucleus of the nucleopulpocytes was stained (i) brown with HES and (ii) pink with AB (spotted arrows). Mucous degeneration was characterised by irregular areas that stained pink with AB. (iv) Some small areas can be noted in the mildly degenerated IVD (stars), (vi) whereas they are abundantly present in the severely degenerated disc. (iv) Granular changes (circles) also appeared with this stain. (vi) The extent of the tissue changes was such that the granules were distributed sparsely and tears were noted (dashed circles) in the most degenerated disc. (iii) Some “ghost cells” (arrowheads) and cell proliferation forming clusters (arrows) could be noted in the mildly degenerated IVD with HES staining. (v) There were almost no cells in the histological samples of the fully degenerated discs (spotted arrows: nucleopulpocytes; stars: mucous degeneration; circles: granular changes; dashed circles: tears; arrowheads: ghost cells; arrows: cell proliferation). (b) The graph represents the variations in the modified Boos scores between skeletally immature (group 1) and skeletally mature (group 2) sheep. Results are expressed as medians. Correlation between the two groups for the modified Boos score was assessed. * $p < 0.05$, statistical difference between two groups.

occurred in ovine. To the best of the authors' knowledge, this is the first study that concomitantly analysed and correlated imaging observations with histological changes related to the spontaneous degeneration that occurred in ageing ovine lumbar IVD according to the second hypothesis. In particular, major changes related to age were observed in lumbar ovine IVDs by 4 years old, when the epiphyseal fusion of the vertebral bodies was complete.

The study assessed the lumbar IVD degeneration in sheep of different ages. Among the various large animal models, the ovine model is commonly used to investigate lumbar IVD degeneration, notably because of its similarities with the human lumbar spine (Daly *et al.*, 2018; Hasler *et al.*, 2010; Lyons *et al.*, 1981; Nisolle *et al.*, 2016; Reid *et al.*, 2002; Reitmaier *et al.*, 2017; Schmidt and Reitmaier, 2013; Schwan *et al.*, 2019; Wilke *et al.*, 1997a; Wilke *et al.*, 1997b). In particular, the human and ovine IVD have a high degree of similarity in terms of water and collagen content, as well as the collagen orientation angle (Lyons *et al.*, 1981; Reid *et al.*, 2002). This parallel between human and ovine IVDs explains why sheep have been widely used as a model to study this tissue and why the present investigation focused on this large-animal model. The human IVD is known to degenerate with age but characterisation of the IVD ageing process in sheep has not been thoroughly documented in the literature. Indeed, most studies that have used sheep as a model induced the degeneration to investigate the IVD changes that occur during this process (Fusellier *et al.*, 2020; Reitmaier *et al.*, 2017). Inducing degeneration is invasive and resource-intensive, while it also implies that the IVD undergoes several injuries and overloading that cannot mimic progressive age-dependent degeneration. Developing new treatment tracks in the field of regenerative medicine

in preclinical studies justifies the objective of finding the most suitable animal model for studying disc degeneration (Fusellier *et al.*, 2020). To investigate such treatments, degenerative discs of preclinical animals are needed, but spontaneous lesions are preferable. For all the studied parameters, significant differences were found between the sheep in group 2, which were more than 4 years old, and in group 1, which comprised skeletally immature sheep. Thus, in the light of the present study, skeletally mature sheep could be a good spontaneous age-related model for research studies of degenerative IVD modalities and for studying biotherapies without the need to induce degeneration. Mild signs of IVD degeneration were observed in young sheep that were 2 or 3 years old. Considering this result, it may be interesting to study the pathophysiological processes occurring during early disc degeneration.

Another similarity with human IVDs that explains the relevance of the present study using sheep as a model is the loss of notochordal cells in the NP with age. The onset of IVD degeneration is caused by different intrinsic and extrinsic factors that induce modifications in the cellular population, particularly in the NP (Colombier *et al.*, 2014). Among the variations that can be observed in cell density in the early stages of the degenerative process, the loss of notochordal cells is predominant. Notochordal cells play a crucial role in the activity and survival of nucleopulpcytes (Erwin *et al.*, 2006; Hunter *et al.*, 2003). Human notochordal cells are lost with skeletal maturity (Butler, 1988; Trout *et al.*, 1982), which results in an imbalance in NP homeostasis and is suspected to be a major event in early NP degeneration. Interestingly, comparison between species has revealed a comparable change in notochordal cells during growth of a 4-year-old mature sheep and chondrodystrophic dogs when compared to the human NP (Hunter *et al.*, 2004). As chondrodystrophic dogs undergo spontaneous IVD degeneration (Bergknut *et al.*, 2012), the authors assumed that a similar process could occur in sheep. Here, and as evidenced by the histological data, the presence of cells exhibiting characteristics similar to those of notochordal cells was noted in group 1, which had not reached complete skeletal maturity. Interestingly, no such cells were observed in the IVD of group 2 sheep, which were more than 4 years old. Thus, the authors hypothesised that these cells could be nests of notochordal cells and that they may disappear at around 4 years of age. Immunohistochemical assessment using specific markers of notochordal cells (*i.e.* CD24, CK-8, CK-18 and GAL3) has confirmed the loss of these cells in ageing human IVD (Liu *et al.*, 2018; Weiler *et al.*, 2010). A study focusing on the presence or absence of these cells in sheep of different ages would be of interest.

In the present study, ovine lumbar IVD degeneration was investigated by MDH, measured as changes detected on X-ray and MR images, and

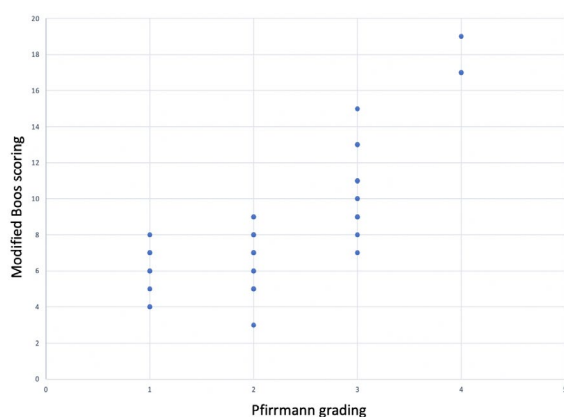


Fig. 6. Modified Boos scoring of the NP according to the Pfirrmann grading. A modified Boos score was applied to the NP of each lumbar ovine IVD and was correlated to the Pfirrmann grade determined on MR images. A positive correlation was found between Boos scores and Pfirrmann grades ($p < 0.0001$, $r_s = 0.84$).

histological alterations were assessed using well-known parameters to investigate IVD degeneration, namely reduction of IVD height, Pfirrmann grade (Pfirrmann *et al.*, 2001) and Boos score (Boos *et al.*, 2002). These parameters are commonly used in IVD disease research studies. Results obtained revealed a substantial inter-rater variability for the Pfirrmann grading, with a κ of 0.64. This value was slightly below the κ reported in the literature (0.69 to 0.81) (Pfirrmann *et al.*, 2001). This could be explained by a certain difficulty to differentiate grade 2 and grade 3, with one observer being slightly more severe than the other (data not shown). Nonetheless, although the inter-observer disagreement was greater than the reference, a difference between two grades was present in only 3 % of all IVDs (2/66), which is close to the reference value of 1.3 % (Pfirrmann *et al.*, 2001). Surprisingly, the modified Pfirrmann grading had a poor intra-rater reliability for one observer (0.88). This value may be explained by the narrow difference that can exist between two grades in this eight-point classification. The consequence of this narrow difference, which makes the modified Pfirrmann grading even more subjective, was reflected by five readings that varied between the two grades for the majority of the IVDs (data not shown). On the other hand, a difference of two grades between the five readings was only found in 3/66 IVDs. The use of these three parameters combined with repetition of data collection for the Pfirrmann grading limited this variation and, thus, bolstered the conclusions.

Modic type 2 changes were observed in sheep of group 2 but there were no Modic type 1 nor type 3 changes. Moreover, Pfirrmann grades > 4 were found in 7 IVDs from group 2, of which 6 were found in the same sheep. It could be assumed that this particular sheep could have exhibited signs of LBP. Yet, surprisingly, the clinical and orthopaedic examinations did not reveal any abnormalities and no history of LBP was reported by the breeder. Numerous studies have assessed and discussed the relationship between LBP and IVD degeneration based on MRI. Among the various imaging parameters, Modic type 1 changes and high Pfirrmann grades have been correlated to LBP (Rahyussalim *et al.*, 2020). Even though changes in the Pfirrmann grading were observed in group 2, Modic type I modifications, which strongly correlate with LBP (Hanumoğlu *et al.*, 2019), were not present. These features suggest that the degenerative lesions were centered on the IVD and that they did not extend to the endplates or the vertebra, which could limit inflammation and pain. Generally, Pfirrmann and Modic type 1 changes are present concomitantly (Yu *et al.*, 2012). The results of the present study suggested the LBP may be more related to endplate inflammatory modifications than strict IVD changes. In animal models, this relationship between IVD degeneration changes and the severity of the clinical signs has not been investigated much, except in a rat

model and transgenic mouse models (Shi *et al.*, 2018). Further studies are needed to establish a scoring that can objectively describe LBP in sheep and to assess whether there is a correlation between LBP and IVD degeneration in this large-animal model.

Histology is considered to be the gold standard for investigating IVD degeneration, although ethical considerations and 3Rs principles favour limiting the number of animals sacrificed for IVD research. Hence, this parameter was included in the present study. Early events of IVD degeneration such as cell modifications mainly occur in the NP, thus the histological analysis focused on this tissue. A strong correlation between imaging findings and histological changes in the NP was found, thus suggesting that imaging modalities could be an alternative to histological assessment of IVD degeneration. However, the study was conducted on a small number of animals. Moreover, in group 1, the number of IVDs which have received a modified Boos score was smaller than the number of IVD assessed by imaging. In contrast, in group 2, all but 1 IVDs were histologically assessed. Yet the number of IVDs assessed by histology in group 1 still remained larger than in group 2 and all the data yielded conclusive and statistically significant results. As the objective of the present study focused on IVD degeneration, which was unlikely to happen in animals of group 1, and in consideration of the 3Rs principles, which aim to reduce the number of animals used in experimental research, it was decided not to euthanise additional animals for the study.

In the present study, T2 relaxation time, also called T2 mapping, correlated with both age and histological data. To increase the sensitivity and accuracy of the results, new imaging methods have been developed to study IVD degeneration. In particular, quantitative methods such as T2 mapping. This method involves determination of the T2 relaxation time, which correlates with the water content of the tissue (Marinelli *et al.*, 2009). In humans, numerous studies have demonstrated the correlation between T2 times and disc degeneration, especially in the early stages (Marinelli *et al.*, 2010; Menezes-Reis *et al.*, 2016; Stelzeneder *et al.*, 2012; Takashima *et al.*, 2012; Yoon *et al.*, 2016). The T2 relaxation time decreases when the disc degenerates, reflecting reductions in water and proteoglycan content of the NP. Only one study to date has performed T2 relaxation time measurements in sheep (Nisolle *et al.*, 2016). Although the same statistical variations were described, with a decrease in the NP T2 time with age, a degree of caution is warranted when comparing the results of the present study with the results of Nisolle *et al.* (2016). Indeed, MRI parameters are not transferable as in the present study the section thickness was half the thickness reported by Nisolle *et al.* (2016) (3 mm *versus* 6 mm, respectively). Moreover, no unit of measure for the relaxation time was specified in Nisolle *et al.* (2016). Furthermore, in the present study, T2 relaxation times

correlated separately with age and Boos scores and these results suggested that T2 relaxation time could be a reliable tool to investigate IVD degeneration in sheep. Moreover, this imaging modality might be a substitute for systematic histological treatment of ovine IVDs. Such an approach could also be useful for longitudinal investigations using MRI-based assessment in regenerative therapy studies. Further studies are needed to develop the quantitative MRI modality to evaluate disc degeneration and to establish reference mapping values in this species.

Conclusions

Sheep undergo spontaneous IVD degeneration, as confirmed by imaging modalities and histological assessment. Experimentally induced IVD degeneration is invasive and resource-intensive (Osti and Vernon-Roberts, 1990). Additionally, a strong correlation between histology and findings from the imaging modalities was found, thus suggesting that this could allow for a reduction in the number of sheep sacrificed for IVD degeneration studies. In particular, the development of quantitative MRI to evaluate progression of IVD degeneration appeared to have ample merit. Thus, further studies are warranted to evaluate the relevance of these new MRI sequences for assessment of IVD degeneration.

Acknowledgments

The authors thank Dominique Rouleau, Ingrid Leborgne, Patrice Roy, Gwenola Touzot-Jourde and Jennifer Flynn for their help with management of the animals during the *in vivo* part of the study, anaesthesia and harvesting of the lumbar spines. The authors thank Dr Chantal Thorin, PhD in Statistics, for the statistical analysis. The authors also thank Sophie Domingues for editing the manuscript.

This research was funded by the ANR Générique 2014 REMEDIV project, the Paris scientifiques region Pays de la Loire 2015 BIO2 project and the ANR JCJC 2016 STIMUDISC project. The authors declare no conflict of interest. The funders had no role in the design of the study; in the collection, analyses or interpretation of the data; in the writing of the manuscript; or in the decision to publish the results.

MF, JC, CLV, AH and JG conceived the study. MF, NB and JC coordinated the study. SM, MF, CD and NB performed the X-ray radiography and MRI. NB and JBH performed the data analysis and the statistical analysis of the imaging data. JL, JA, NB, CD and JBH performed the histological staining and the Boos score analysis. NB, JBH and CD wrote the paper. MF, JC, JA, SM, JL and AH helped with the writing and reviewing of the manuscript. JG and CLV helped writing of the paper, approved the final version and obtained the funding.

References

- Adams MA, Roughley PJ (2006) What is intervertebral disc degeneration, and what causes it? *Spine (Phila Pa 1976)* **31**: 2151-2161.
- Alini M, Eisenstein SM, Ito K, Little C, Kettler AA, Masuda K, Melrose J, Ralphs J, Stokes I, Wilke HJ (2008) Are animal models useful for studying human disc disorders/degeneration? *Eur Spine J* **17**: 2-19.
- Barone R (2010) Anatomie comparée des mammifères domestiques. Tome 1 - Ostéologie 5th edition. Ed Vigot.
- Bergknut N, Rutges JPHJ, Kranenburg HJC, Smolders LA, Hagman R, Smidt HJ, Lagerstedt AS, Penning LC, Voorhout G, Hazewinkel HAW, Grinwis GCM, Creemers LB, Meij BP, Dhert WJA (2012) The dog as an animal model for intervertebral disc degeneration? *Spine (Phila Pa 1976)* **37**: 351-358.
- Boos N, Weissbach S, Rohrbach H, Weiler C, Spratt KF, Nerlich AG (2002) Classification of age-related changes in lumbar intervertebral discs: 2002 Volvo Award in basic science. *Spine (Phila Pa 1976)* **27**: 2631-2644.
- Butler WF (1988) Comparative anatomy and development of the mammalian disc. In: *The Biology of the Intervertebral Disc*. pp: 83-108.
- Clouet J, Fusellier M, Camus A, Le Visage C, Guicheux J (2019) Intervertebral disc regeneration: From cell therapy to the development of novel bioinspired endogenous repair strategies. *Adv Drug Deliv Rev* **146**: 306-324.
- Clouet J, Pot-Vaucel M, Grimandi G, Masson M, Lesoeur J, Fellah BH, Gauthier O, Fusellier M, Cherel Y, Maugars Y, Guicheux J, Vinatier C (2011) Characterization of the age-dependent intervertebral disc changes in rabbit by correlation between MRI, histology and gene expression. *BMC Musculoskeletal Disord* **12**: 147. DOI: 10.1186/1471-2474-12-147.
- Colombier P, Clouet J, Hamel O, Lescaudron L, Guicheux J (2014) The lumbar intervertebral disc: from embryonic development to degeneration. *Joint Bone Spine* **81**: 125-129.
- Craig Platenberg R, Hubbard GB, Ehler WJ, Hixson CJ (2001) Spontaneous disc degeneration in the baboon model: magnetic resonance imaging and histopathologic correlation. *J Med Primatol* **30**: 268-272.
- Daly CD, Ghosh P, Badal T, Shimmon R, Jenkin G, Oehme D, Cooper-White J, Sher I, Chandra R V., Goldschlager T (2018) A comparison of two ovine lumbar intervertebral disc injury models for the evaluation and development of novel regenerative therapies. *Global Spine J* **8**: 847-859.
- Daly C, Ghosh P, Jenkin G, Oehme D, Goldschlager T (2016) A review of animal models of intervertebral disc degeneration: pathophysiology, regeneration, and translation to the clinic. *Biomed Res Int* **2016**: 5952165. DOI: 10.1155/2016/5952165.
- De Schepper EIT, Damen J, Van Meurs JBJ, Ginai AZ, Popham M, Hofman A, Koes BW, Bierma-

Zeinstra SM (2010) The association between lumbar disc degeneration and low back pain: the influence of age, gender, and individual radiographic features. *Spine (Phila Pa 1976)* **35**: 531-536.

Dieleman JL, Baral R, Birger M, Bui AL, Bulchis A, Chapin A, Hamavid H, Horst C, Johnson K, Joseph J, Lavado R, Lomsadze L, Squires E, Campbell M, Decenso B, Flaxman AD, Gabert R, Highfill T, Nightingale N, Templin T, Tobias MI, Vos T, Murray CJL (2017) The State of US Health, 1990-2010: burden of diseases, injuries and risk factors. *JAMA* **316**: 2627-2646.

Erwin WM, Ashman K, O'Donnel P, Inman RD (2006) Nucleus pulposus notochord cells secrete connective tissue growth factor and up-regulate proteoglycan expression by intervertebral disc chondrocytes. *Arthritis Rheum* **54**: 3859-3867.

Fusellier M, Clouet J, Gauthier O, Tryfonidou M, Le Visage C, Guicheux J (2020) Degenerative lumbar disc disease: *in vivo* data support the rationale for the selection of appropriate animal models. *Eur Cells Mater* **39**: 18-47.

Geurts JW, Willems PC, Kallewaard JW, Van Kleef M, Dirksen C (2018) The impact of chronic discogenic low back pain: costs and patients' burden. *Pain Res Manag* **2018**: 4696180. DOI: 10.1155/2018/4696180.

Griffith JF, Wang YXJ, Antonio GE, Choi KC, Yu A, Ahuja AT, Leung PC (2007) Modified Pfirrmann grading system for lumbar intervertebral disc degeneration. *Spine (Phila Pa 1976)* **32**: E708-712. DOI: 10.1097/BRS.0b013e31815a59a0.

Gruber HE, Johnson T, Norton HJ, Hanley EN (2002) The sand rat model for disc degeneration: radiologic characterization of age-related changes: cross-sectional and prospective analyses. *Spine (Phila Pa 1976)* **27**: 230-234.

Hanımoğlu H, Çevik S, Yılmaz H, Kaplan A, Çalış F, Katar S, Evran Ş, Akkaya E, Karaca O (2019) Effects of Modic type 1 changes in the vertebrae on low back pain. *World Neurosurg*. **121**: e426-e432.

Hasler C, Sprecher CM, Milz S (2010) Comparison of the immature sheep spine and the growing human spine: a spondylometric database for growth modulating research. *Spine (Phila Pa 1976)* **35**: E1262-1272.

Hoy D, March L, Brooks P, Blyth F, Woolf A, Bain C, Williams G, Smith E, Vos T, Barendregt J, Murray C, Burstein R, Buchbinder R (2014) The global burden of low back pain: estimates from the global burden of disease 2010 study. *Ann Rheum Dis* **73**: 968-974.

Hunter CJ, Matyas JR, Duncan NA (2003) The notochordal cell in the nucleus pulposus: A review in the context of tissue engineering. *Tissue Eng*. **9**: 667-677.

Hunter CJ, Matyas JR, Duncan NA (2004) Cytomorphology of notochordal and chondrocytic cells from the nucleus pulposus: a species comparison. *J Anat* **205**: 357-362.

Kawamoto T, Shimizu M (2000) A method for preparing 2-to 50-µm-thick fresh-frozen sections

of large samples and undecalcified hard tissues. *Histochem Cell Biol* **113**: 331-339.

Khan AN, Jacobsen HE, Khan J, Filippi CG, Levine M, Lehman RA, Riew KD, Lenke LG, Chahine NO (2017) Inflammatory biomarkers of low back pain and disc degeneration: a review. *Ann N Y Acad Sci* **1410**: 68-84.

Kigozi J, Konstantinou K, Ogollah R, Dunn K, Martyn L, Jowett S (2019) Factors associated with costs and health outcomes in patients with back and leg pain in primary care: a prospective cohort analysis. *BMC Health Serv Res* **19**: 406. DOI: 10.1186/s12913-019-4257-0.

Lee K, Shin JS, Lee J, Lee YJ, Kim MR, Seong I, Jun J, Park KB, Ha IH (2017) Lumbar intervertebral disc space height in disc herniation and degeneration patients aged 20 to 25. *Int J Clin Exp Med* **10**: 6828-6836.

Liu Z, Zheng Z, Qi J, Wang J, Zhou Q, Hu F, Liang J, Li C, Zhang W, Zhang X (2018) CD24 identifies nucleus pulposus progenitors/notochordal cells for disc regeneration. *J Biol Eng* **12**: 35. DOI: 10.1186/s13036-018-0129-0.

Lucas O, Hamel O, Blanchais A, Lesoeur J, Abadie J, Fella BH, Fusellier M, Gauthier O, Bord E, Grimandi G, Vinatier C, Guicheux J, Clouet J (2012) Laser-treated nucleus pulposus as an innovative model of intervertebral disc degeneration. *Exp Biol Med* **237**: 1359-1367.

Luoma K, Riihimäki H, Luukkonen R, Raininko R, Viikari-Juntura E, Lamminen A (2000) Low back pain in relation to lumbar disc degeneration. *Spine (Phila Pa 1976)* **25**: 487-492.

Lyons G, Eisenstein SM, Sweet MBE (1981) Biochemical changes in intervertebral disc degeneration. *Biochim Biophys Acta* **673**: 443-453.

Marinelli NL, Haughton VM, Anderson PA (2010) T2 relaxation times correlated with stage of lumbar intervertebral disk degeneration and patient age. *AJNR Am J Neuroradiol* **31**: 1278-1282.

Marinelli NL, Haughton VM, Muñoz A, Anderson PA (2009) T2 relaxation times of intervertebral disc tissue correlated with water content and proteoglycan content. *Spine (Phila Pa 1976)*. **34**: 520-524.

Menezes-Reis R, Salmon CEG, Bonugli GP, Mazoroski D, Tamashiro MH, Savarese LG, Nogueira-Barbosa MH (2016) Lumbar intervertebral discs T2 relaxometry and T1ρ relaxometry correlation with age in asymptomatic young adults. *Quant Imaging Med Surgery* **6**: 402-412.

Modic MT (2007) Lumbar degenerative disk. *Radiology* **245**: 43-61.

Moran NC, O'Connor TP (1994) Age attribution in domestic sheep by skeletal and dental maturation: a pilot study of available sources. *Int J Osteoarchaeol*. DOI: 10.1002/oa.1390040402.

Nisolle JF, Bihin B, Kirschvink N, Neveu F, Clegg P, Dugdale A, Wang X, Vandeweerdt JM (2016) Prevalence of age-related changes in ovine lumbar intervertebral discs during computed tomography

and magnetic resonance imaging. *Comp Med* **66**: 300-307.

Nuckley DJ, Kramer PA, Del Rosario A, Fabro N, Baran S, Ching RP (2008) Intervertebral disc degeneration in a naturally occurring primate model: radiographic and biomechanical evidence. *J Orthop Res* **26**: 1283-1288.

Ohnishi T, Sudo H, Tsujimoto T, Iwasaki N (2018) Age-related spontaneous lumbar intervertebral disc degeneration in a mouse model. *J Orthop Res* **36**: 224-232.

Osti OL, Vernon-Roberts B (1990) Volvo Award in experimental studies. Anulus tears and intervertebral disc degeneration. An experimental study using an animal model. *Spine (Phila Pa 1976)* **15**: 762-767.

Pennicooke B, Hussain I, Berlin C, Sloan SR, Borde B, Moriguchi Y, Lang G, Navarro-Ramirez R, Cheetham J, Bonassar LJ, Härtl R (2018) Annulus fibrosus repair using high-density collagen gel. *Spine (Phila Pa 1976)* **43**: E208-E215.

Pfirrmann CWA, Metzendorf A, Zanetti M, Hodler J, Boos N (2001) Magnetic resonance classification of lumbar intervertebral disc degeneration. *Spine (Phila Pa 1976)* **26**: 1873-1878.

Pinheiro J, Bates D (2000) Mixed-effects models in S and S-PLUS. Ed Springer-Verlag, New York.

Rahyussalim AJ, Zufar MLL, Kurniawati T (2020) Significance of the association between disc degeneration changes on imaging and low back pain: a review article. *Asian Spine J* **14**: 245-257.

Ravindra VM, Senglaub SS, Rattani A, Dewan MC, Härtl R, Bisson E, Park KB, Shrimme MG (2018) Degenerative lumbar spine disease: estimating global incidence and worldwide volume. *Global Spine J* **8**: 784-794.

Reid JE, Meakin JR, Robins SP, Skakle JMS, Hukins DWL (2002) Sheep lumbar intervertebral discs as models for human discs. *Clin Biomech* **17**: 312-314.

Reitmaier S, Graichen F, Shirazi-Adl A, Schmidt H (2017) Separate the sheep from the goats: use and limitations of large animal models in intervertebral disc research. *J Bone Joint Surg Am* **99**: e102. DOI: 10.2106/JBJS.17.00172.

Schmidt H, Reitmaier S (2013) Is the ovine intervertebral disc a small human one? A finite element model study. *J Mech Behav Biomed Mater* **17**: 229-241.

Schwan S, Ludtka C, Friedmann A, Heilmann A, Baerthel A, Brehm W, Wiesner I, Meisel HJ, Goehre F (2019) Long-term pathology of ovine lumbar spine degeneration following injury *via* percutaneous minimally invasive partial nucleotomy. *J Orthop Res* **37**: 2376-2388.

Sheng SR, Wang XY, Xu HZ, Zhu GQ, Zhou YF (2010) Anatomy of large animal spines and its comparison to the human spine: a systematic review. *Eur Spine J* **19**: 46-56.

Shi C, Das V, Li X, Kc R, Qiu S, O-Sullivan IS, Ripper RL, Kroin JS, Mwale F, Wallace AA, Zhu B, Zhao L, van Wijnen AJ, Ji M, Lu J, Votta-Velis G, Yuan W, Im HJ (2018) Development of an *in vivo* mouse model of discogenic low back pain. *J Cell Physiol* **233**: 6589-6602.

Singh K, Masuda K, An HS (2005) Animal models for human disc degeneration. *Spine J* **5**: 267S-279S.

Sloan SR, Wipplinger C, Kirnaz S, Navarro-Ramirez R, Schmidt F, McCloskey D, Pannellini T, Schiavinato A, Härtl R, Bonassar LJ (2020) Combined nucleus pulposus augmentation and annulus fibrosus repair prevents acute intervertebral disc degeneration after discectomy. *Sci Transl Med* **12**: eaay2380. DOI: 10.1126/scitranslmed.aay2380.

Stelzeneder D, Welsch GH, Kovács BK, Goed S, Paternostro-Sluga T, Vlychou M, Friedrich K, Mamisch TC, Trattnig S (2012) Quantitative T2 evaluation at 3.0T compared to morphological grading of the lumbar intervertebral disc: a standardized evaluation approach in patients with low back pain. *Eur J Radiol* **81**: 324-330.

Takashima H, Takebayashi T, Yoshimoto M, Terashima Y, Tsuda H, Ida K, Yamashita T (2012) Correlation between T2 relaxation time and intervertebral disk degeneration. *Skeletal Radiol* **41**: 163-167.

Trout JJ, Buckwalter JA, Moore KC, Landas SK (1982) Ultrastructure of the human intervertebral disc. I. Changes in notochordal cells with age. *Tissue Cell* **14**: 359-369.

Wang F, Cai F, Shi R, Wang XH, Wu XT (2016) Aging and age related stresses: a senescence mechanism of intervertebral disc degeneration. *Osteoarthritis Cartilage* **24**: 398-408.

Weiler C, Nerlich AG, Schaaf R, Bachmeier BE, Wuertz K, Boos N (2010) Immunohistochemical identification of notochordal markers in cells in the aging human lumbar intervertebral disc. *Eur Spine J* **19**: 1761-1770.

Wilke HJ, Kettler A, Claes LE (1997a) Are sheep shines a valid biomechanical model for human spines? *Spine (Phila Pa 1976)* **22**: 2365-2374.

Wilke HJ, Kettler A, Wenger KH, Claes LE (1997b) Anatomy of the sheep spine and its comparison to the human spine. *Anat Rec* **247**: 542-555.

Yoon MA, Hong SJ, Kang CH, Ahn KS, Kim BH (2016) T1rho and T2 mapping of lumbar intervertebral disc: correlation with degeneration and morphologic changes in different disc regions. *Magn Reson Imaging* **34**: 932-939.

Editor's note: There were no questions from reviewers for this paper, therefore there is no Discussion with Reviewers section. The Scientific Editor responsible for this paper was Sibylle Grad.